Uncertainty Reduction of Damage Growth Properties Using Structural Health Monitoring

Alexandra Coppe,* Raphael T. Haftka,† and Nam H. Kim‡
University of Florida, Gainesville, Florida 32611
and
Fuh-Gwo Yuan§
North Carolina State University, Raleigh, North Carolina 27695

Structural health monitoring provides sensor data that can monitor fatigue-induced damage in service. This information may in turn be used to improve the characterization of material properties that govern damage growth for the structure being monitored. These properties are often widely distributed among nominally identical materials because of differences in manufacturing processes and due to aging effects. Improved accuracy in damage growth characteristics would allow more accurate prediction of the remaining useful life of the structural component. In this paper, a probabilistic approach using Bayesian inference is employed to progressively reduce the uncertainty in structure-specific damage growth parameters in spite of noise and bias in sensor measurements. Starting from an initial wide distribution of damage growth parameters that are obtained from coupon tests, the distribution is progressively narrowed using damage growth data between consecutive measurements. Detailed discussions on how to construct the likelihood function under the given noise of sensor data and how to update the distribution are presented. The approach is applied to simulated damage growth in fuselage panels due to cycles of pressurization. It is shown that the proposed method rapidly converges to the accurate damage growth parameters when the initial damage size is relatively large: e.g., 20 mm. Fairly accurate damage growth parameters are obtained even with measurement errors of 5 mm. Using the identified damage growth parameters, it is shown that the 95% conservative remaining useful life converges to the true remaining useful life from the conservative side. The proposed approach may have the potential of turning aircraft into flying fatigue laboratories.

Nomenclature

a	=	half-crack size
a_C	=	critical half-crack size
a_N	=	half-crack size at Nth inspection
a_{true}	=	true half-crack size
a_1	=	initial half-crack size
a^{meas}	=	measured half-crack size
a_N^{sim}	=	estimated true damage size
b	=	bias in damage-size measurement
C	=	Paris law parameter
d	=	difference between measured and estimated damage growth
e_N^{sim}	=	simulated error in measurements
F_{meas}	=	cumulative distribution function of measured damage growth
f_{ini}	=	initial (or prior) probability density function
$f_{i,\text{test}}$	=	likelihood function
f_{sim}	=	probability density function of estimated damage growth
f_{updt}	=	updated (or posterior) probability density function
K_{IC}	=	fracture toughness
M	=	Monte Carlo simulation sample size
m	=	Paris law exponent
N	=	step between inspections
p	=	pressure
r	=	fuselage radius
t	=	panel thickness
V	=	range of noise in damage-size measurement
v	=	noise in damage-size measurement
Δa	=	crack growth
Δa_N	=	damage growth at Nth cycle
Δa^{meas}	=	measured crack growth
Δa_N^{sim}	=	estimated true damage growth
Δe_N^{sim}	=	estimated error in the damage growth
ΔK	=	range of stress intensity factor
σ	=	applied stress

*Graduate Student, Department of Mechanical and Aerospace Engineering; alex.coppe@ufl.edu. Student Member AIAA.
†Distinguished Professor, Department of Mechanical and Aerospace Engineering; haftka@ufl.edu. Fellow AIAA.
‡Associate Professor, Department of Mechanical and Aerospace Engineering; nkim@ufl.edu. Member AIAA.
§Department of Mechanical and Aerospace Engineering; yuan@ncsu.edu. Associate Fellow AIAA.

I. Introduction

STRUCTURAL health monitoring (SHM) may have significant impacts on increasing safety as well as reducing the operating and maintenance costs of structures by providing an accurate quantification of degradation and damage at an early stage to reduce or eliminate malfunctions. Furthermore, SHM can allow damage diagnosis that will provide the structural health status that in conjunction with prognosis will help predictions of the remaining useful life (RUL) without intrusive and time consuming inspections. Continual online SHM is based on dynamic processes through the diagnosis of early damage detection, then prognosis of health status and remaining life.

Once the damage reaches a detectable size, various SHM techniques can be employed to evaluate the current state of structural health by measuring the size of the damage [1]. In physics-based prognosis techniques, it is necessary to incorporate the measured data into a damage growth model to predict the future behavior of the damage.

Prognosis techniques can be categorized based on the usage of information: 1) physics-based, 2) data-driven, and 3) hybrid methods. The physics-based method, or model-based method [2], assumes that the physical model that governs the structure's behavior is known and uses sensor data to identify the physical model parameters. The dynamic stochastic equation, lumped-parameter model [3], and functional models [4] belong to this category. In the case of SHM, a crack growth model [3,5,6] and spall growth models are often used for micro levels, and first-principle models [7] are used for macro levels.

The data-driven method [8] uses information from collected data to predict the future status of the system and includes least-squares regression [9,10], Gaussian process regression [11,12], neural network [7,11,12], and relevance vector machine [11,13]. This method has advantages when the structure's behavior is so complex that no simple physical model is available. Although the data-driven method may be more accurate in early stages, the physics-based model becomes more accurate as more data are used to identify the physical parameters. The hybrid method [14] uses the advantages from both methods and includes the particle filtering method [15] and Bayesian techniques [16,17].

It is generally accepted that uncertainty is the most challenging aspect in prognosis [17,18]. Sources of uncertainty are from initial state estimation, current state estimation, failure threshold, sensor measurement, future load, future environment, and models. To address the uncertainty, various methods have been proposed, such as confidence intervals [19], relevance vector machine [11], Gaussian process regression [11,12], and particle filters [15,20]. Bayesian methods have become popular in the past years but are mainly used to extrapolate the crack behavior by updating the crack size distribution rather than the material properties. Although the crack size distribution is important to diagnose the current health status, the crack growth properties of the material are more important for the purpose of prognosis. The objective of this paper is to characterize the crack growth properties as an intermediate step toward predicting the RUL of the structure, which will allow us to improve our knowledge of the entire structure rather than the specific damage that is being monitored.

The current technology of diagnosis and prognosis using sensor-based SHM has difficulties associated with uncertainties in sensor data, damage growth models, and material and geometric properties. The first is related to identifying the current health status, while the others are related to predicting the health status in the future. Uncertainties in sensor data can be classified into two categories: systematic departure due to bias and random variability due to noise. The former is caused by calibration error, sensor location, and device error, while the latter is caused by measurement environment. Note that bias may tend to vary as the crack grows due to the nature of the error; for example, the sensors located in the parallel direction to the crack growth direction tend to have larger error than those located in the perpendicular direction. In this paper, however, it is assumed that the bias is constant over the entire life of the structure.

Compared to manual inspections [nondestructive inspection/ evaluation (NDI/E) techniques], the accuracy of SHM is relatively poor. The minimum detectable size of damage using SHM is much larger than that of NDI/E methods. In addition, the measured data have the aforementioned noise and bias. Thus, the major challenge in SHM-based prognosis is how to accurately predict the damage growth when the measured data include both noise and bias. Although noise is commonly discussed, bias is often ignored in literature. However, unlike manual inspection, SHM may provide frequent measurements of damage, making it possible to track damage growth. This, in turn, can reduce the uncertainty in the material properties that govern damage growth. The uncertainty in these properties is normally large because of variability in manufacturing and aging of the structure. The main objective of this paper is to demonstrate the reduction in uncertainty of these parameters using an abundance of SHM data, although they include noise and bias. In other words, numerous data obtained from SHM can be used to characterize damage growth behaviors of a specific structure. A statistical approach using Bayesian inference is employed to progressively improve the accuracy of predicting damage growth parameters under noise and bias of sensor measurements.

The proposed approach is demonstrated using a through-the-thickness crack in an aircraft fuselage panel which grows through cycles of pressurization. A simple damage growth model [21] with two damage growth parameters is used. However, more advanced damage growth models can also be used, which usually come with more parameters. Using this simple model, the goal is to demonstrate that noisy SHM data can be used to identify the damage growth parameters of the monitored panel. This process can be viewed as turning every aircraft into a flying fatigue laboratory. Reducing uncertainty in damage growth parameters can in turn reduce the uncertainty in predicting RUL: i.e., prognosis. Improved knowledge of RUL can have practical consequences such as increased time between visual inspections or a reduction in hardware testing when SHM is combined with manual inspection.

The paper is organized as follows. In Sec. II, a simple damage growth model based on the Paris model is presented. In Sec. III the measurement model used in this paper is introduced and shows how error in measurements due to SHM is added to the model presented in the previous section. It also presents how Bayesian inference is used to identify damage growth parameters. In Sec. IV the numerical application of the model is presented. In Sec. V, the updating of damage parameter m is presented as well as the resulting prognosis. In Sec. VI, results similar to those presented in Sec. V but obtained by updating the other damage parameter, C, are presented. Conclusions are presented in Sec. VII along with future plans.

II. Damage Growth Model

Damage in a structure starts at a microstructure level, such as dislocations, and gradually grows to the level of detectable macrocracks through nucleation and growth. Initial microdamage grows slowly, is often difficult to detect, and is not dangerous for structural safety. Thus, SHM often focuses on macrocracks, which grow relatively quickly due to fatigue loadings.

In this paper, we consider fatigue crack growth in a fuselage panel with initial half-crack size a_i subjected to fatigue loading with constant amplitude due to pressurization. The hoop stress varies between a maximum value of σ and a minimum value of zero in one flight. One cycle of fatigue loading represents one flight. As used by many other researchers [22,23], the following Paris law is used for the damage growth model [21]:

$$\frac{da}{dN} = C(\Delta K)^m \qquad (1)$$

where a is the half-crack size in meters, N is the number of cycles (flights), da/dN is the crack growth rate in meters/cycle, and ΔK is the range of stress intensity factor in MPa$\sqrt{\text{meter}}$. The above model has two damage growth parameters: C and m.

The range ΔK of stress intensity factor for a center-cracked panel is calculated as a function of the stress σ and the half-crack length a in Eq. (2), and the hoop stress due to the pressure differential Δp is given by Eq. (3):

$$\Delta K = \sigma \sqrt{\pi a} \qquad (2)$$

$$\sigma = \frac{(\Delta p) r}{t} \qquad (3)$$

where r is the fuselage radius, and t is the panel thickness. Equation (2) does not include a geometric correction factor due to the finite size of the panel, and Eq. (3) does not include corrections due to the complexity of the fuselage construction, so that they are both approximate.

The number of cycles N of fatigue loading that makes a crack grow from the initial half-crack size a_i to the final half-crack a_N can be obtained by integrating Eq. (1) as

$$N = \int_{a_i}^{a_N} \frac{\mathrm{d}a}{C(\sigma\sqrt{\pi a})^m} = \frac{a_N^{1-\frac{m}{2}} - a_i^{1-\frac{m}{2}}}{C(1-\frac{m}{2})(\sigma\sqrt{\pi})} \qquad (4)$$

Alternatively, the half-crack size a_N after N cycles of fatigue loading can be obtained by solving Eq. (4) for a_N as

$$a_N = \left(NC\left(1-\frac{m}{2}\right)(\sigma\sqrt{\pi})^m + a_i^{1-\frac{m}{2}}\right)^{\frac{2}{2-m}} \qquad (5)$$

The panel will fail when the crack reaches a critical half-crack size a_C. Here, we assume that this critical crack size is when the stress intensity factor exceeds the plane-strain fracture toughness K_{IC}. This leads to the following expression for the critical crack size (again neglecting finite panel effects):

$$a_c = \left(\frac{K_{IC}}{\sigma\sqrt{\pi}}\right)^2 \qquad (6)$$

III. Statistical Characterization of Damage Growth Properties Using Bayesian Inference

Damage growth parameters C and m are critical factors to determine the growth of damage. These parameters are normally estimated by fitting fatigue test data under a controlled laboratory environment. However, uncertainty in these parameters is normally large not only at a material level because of variability in manufacturing and aging of the specific panel, but also at a specimen level because of variability related to testing processes. However, a specific panel in an airplane may have a much narrower distribution of damage growth parameters or even have deterministic values. In this section, Bayesian inference will be used to identify these panel-specific parameters.

As can be seen in Fig. 1, the exponent m is the slope of the fatigue crack curve in the log–log scale, while the parameter C corresponds to the y intercept at $\Delta K = 1$, of the fatigue curve. To simplify the presentation, it is assumed that the parameter C has a known deterministic value, and thus uncertainty is only in m. However, the uncertainty in C can also be considered in the same way. From the scattered coupon test data, the upper and lower bounds of m can be estimated using log–log plots of crack growth rate illustrated in Fig. 1. Since prior knowledge is limited, we assume that m is uniformly distributed between these two bounds. Then the goal is to narrow the distribution of the exponent using Bayesian inference with measured damage growth.

Since the Paris model is based on crack growth, we use the measured crack growth data from the diagnosis to characterize the damage growth parameters. Let measurements be performed at every ΔN, and let N be the current cycle. The half-crack growth between two measurements can be defined as

$$\Delta a_N^{\mathrm{meas}} = a_N^{\mathrm{meas}} - a_{N-\Delta N}^{\mathrm{meas}} \qquad (7)$$

Bayesian inference is based on the Bayes theorem of conditional probability. It is used to obtain the updated (also called posterior)
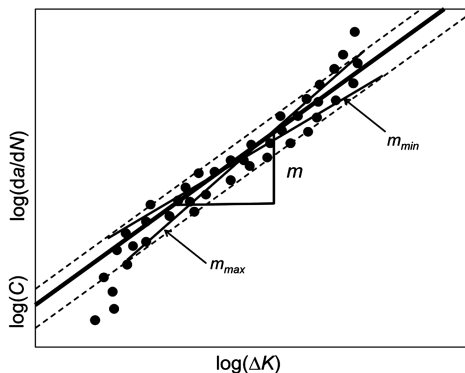

Fig. 1 Illustration of the estimation of Paris model parameters using a log–log plot of crack growth rate.

probability of a random variable by using new information available for the variable. In this paper, since the probability distribution of m given Δa is of interest, we use the following form of the Bayes theorem [24]:

$$f_{\mathrm{updt}}(m) = \frac{l(\Delta a|m)f_{\mathrm{ini}}(m)}{\int_{-\infty}^{+\infty} l(\Delta a|m)f_{\mathrm{ini}}(m)\,\mathrm{d}m} \qquad (8)$$

where $f_{\mathrm{ini}}(m)$ is the assumed (or prior) probability density function (PDF) of m, $f_{\mathrm{updt}}(m)$ is the updated (or posterior) PDF of m, and $l(\Delta a|m)$ is called a likelihood function, which is the probability of obtaining the measured damage growth Δa for a given value of m. The denominator in Eq. (8) can be considered as a normalizing constant that makes $f_{\mathrm{updt}}(m)$ to satisfy the property of PDF. Since $f_{\mathrm{ini}}(m)$ is given or assumed, the most important step in Bayesian inference is to calculate the likelihood function, which determines the uncertainty structure of the posterior distribution. In the literature, the likelihood function is often assumed to be Gaussian or to have analytical expressions. This assumption is made not because of physics but because of convenience. Since the posterior distribution strongly depends on the likelihood function, any assumptions about the likelihood function may lead to errors in posterior distribution. The main contribution of this paper is to rigorously show the process of calculating the likelihood function by propagating uncertainties through the physical model.

The likelihood function is designed to integrate the information obtained from SHM measurements to the knowledge about the distribution of m. The physical interpretation of the likelihood is the PDF value of the true crack growth at the measured crack growth for given m. Although the true crack growth would be a single value, it is considered to be randomly distributed in the viewpoint of measured crack growth due to various uncertainties in the process. Thus, it is important to estimate the distribution of true crack growth. In general, the measured crack growth includes the effect of bias and noise of the sensor measurement as well as uncertainty in input loads.

In this paper, instead of using measured crack growth data, simulated crack growth data are used with appropriate models of noise and bias. The process will be repeated to estimate the statistical characteristics of real measurements. Let a_N be the true half-crack size, let b be the bias, and let v_N be the noise at the current cycle N. The true crack sizes are simulated using the true values of parameters m_{true} and C_{true} from Eq. (5). The measured crack sizes $2a_N^{\mathrm{meas}}$ are then simulated as

$$2a_N^{\mathrm{meas}} = 2a_N + b + v_N \qquad (9)$$

The measurement bias b reflects a deterministic bias, such as calibration error, while the noise v_N reflects random noise. For subsequent simulated measurements, the bias b remains constant, while the noise v_N is uniformly distributed within the range of $[-V, +V]$. Once the measure crack sizes are simulated using Eq. (9), the true crack size a_N is not used in damage growth parameter identification. Then the goal is to estimate m^{true} using the measured crack growth.

The expression in Eq. (9) can be used to define the crack growth between two consecutive SHM measurements as follows:

$$\Delta a_N^{\mathrm{meas}} = a_N^{\mathrm{meas}} - a_{N-\Delta N}^{\mathrm{meas}} = \Delta a_N + \Delta v_N \qquad (10)$$

where Δa_N is the true crack growth and $\Delta v_N = v_N - v_{N-\Delta N}$ is the difference between two random noises. Although v_N and $v_{N-\Delta N}$ have the same range of $[-V, +V]$, they are independent.

At a given SHM measurement, the measured crack size in Eq. (9) has the same distribution type as the noise, while the measured crack growth in Eq. (10) has the same distribution type as Δv_N. Since there is no information regarding the distribution of noise, in this paper it is assumed to be uniformly distributed with mean at zero. Thus, the measured crack size is also uniformly distributed. On the other hand, it can be easily shown that Δv_N is triangularly distributed with mean at zero. Consequently, the crack growth is also triangularly distributed with the mean at Δa_N. Thus, the respective distributions can be defined as

$$\begin{cases} a_N^{\text{meas}} \sim \text{uniform}(a_N + b/2 - V/2; a_N + b/2 + V/2) \\ \Delta a_N^{\text{meas}} \sim \text{triangular}(\Delta a_N - V; \Delta a_N; \Delta a_N + V) \end{cases} \quad (11)$$

The quantities defined above only involve measurement error. In general, however, the crack growth model may also have modeling error, which is related to numerical simulation. To calculate the likelihood function, we introduce a simulated half-crack size a_N^{sim} that involves a modeling error $e_N^{\text{sim}}(m)$ as

$$a_N^{\text{sim}}(m) = a_N + e_N^{\text{sim}}(m) \quad (12)$$

We use the superscript sim for modeling error, because it also includes propagated uncertainty through numerical simulation. The simulated crack size depends on Paris parameters m and C as well as the initial crack size, but only uncertainty in m is considered. Similarly, the simulated crack growth can be written as

$$\Delta a_N^{\text{sim}}(m) = \Delta a_N + \Delta e_N^{\text{sim}}(m) \quad (13)$$

Different from measurement errors, the uncertainty in Δe_N^{sim} is not well characterized; it often requires Monte Carlo simulation (MCS) through the physics model that governs the crack growth.

The idea of calculating likelihood is to identify the damage growth parameter by comparing the measured crack growth, Δa_N^{meas}, with the simulated crack growth, Δa_N^{sim}, with a given m. The difference between these two growths can be defined as

$$d(m) = \Delta a_N^{\text{sim}}(m) - \Delta a_N^{\text{meas}} \quad (14)$$

If the analytical PDFs of Δa_N^{meas} and Δa_N^{sim} are available, then the PDF of d can readily be calculated. The likelihood $l(\Delta a | m)$ is then defined as the value of this PDF at $d(m) = 0$. Since, in general, the analytical PDFs are not available, the MCS is used to calculate the likelihood. Since MCS is a discrete process, it is not trivial to calculate the PDF directly. Instead, the probability of $|d| \leq \epsilon$ with ϵ being a small constant is used as a definition of likelihood:

$$l(\Delta a | m) = P(|d| \leq \epsilon) \quad (15)$$

Note that if the right-hand side is divided by 2ϵ and if ϵ approaches zero, then the likelihood becomes the value of PDF at $d(m) = 0$. In the viewpoint of Eq. (8), since the posterior distribution will be normalized, the above definition works for likelihood although it is given in the form of probability.

If the likelihood $l(\Delta a | m)$ is purely calculated by sampling Δa_N^{meas} and Δa_N^{sim}, the tolerance ϵ needs to be large enough to include enough samples to reduce sampling errors. On the other hand, if ϵ is too large, errors will be incurred due to nonlinearity in the likelihood function.

In general, since the measurement error that controls Δa_N^{meas} is independent of the modeling error that controls Δa_N^{sim}, the separable sampling scheme can be performed, and samples of in Eq. (14) can be calculated by comparing all possible combinations of the two sets of samples [25]. In addition, computational efficiency can significantly be improved since the analytical PDF of Δa_N^{meas} is available from Eq. (11). The PDF of Δa_N^{sim} is not available analytically, because it is obtained by propagating uncertainties through the crack growth model.

The definition of likelihood in Eq. (15) can be expanded by

$$l(\Delta a | m) = P(|d| \leq \epsilon) = P(d + \epsilon \geq 0) - P(d - \epsilon \geq 0) \quad (16)$$

Using conditional expectation on the second term on the right-hand side, we obtain

$$P(d - \epsilon \geq 0) = P(\Delta a_N^{\text{sim}} - \Delta a_N^{\text{meas}} - \epsilon \geq 0)$$

$$= \int_{\Delta a_N^{\text{sim}}} P(\Delta a_N^{\text{sim}} - \Delta a_N^{\text{meas}} - \epsilon \geq 0) f_{\text{sim}}(\Delta a_N^{\text{sim}}) \, d\Delta a_N^{\text{sim}}$$

$$= \int_{\Delta a_N^{\text{sim}}} F_{\text{meas}}(\Delta a_N^{\text{sim}} - \epsilon) f_{\text{sim}}(\Delta a_N^{\text{sim}}) \, da_N^{\text{sim}} \quad (17)$$

where $f_{\text{sim}}(x)$ is the PDF of Δa_N^{sim} and $F_{\text{meas}}(x)$ is the cumulative distribution function (CDF) of Δa_N^{meas}. The last relation is obtained

from the definition of CDF: i.e., by considering Δa_N^{meas} as the only random variable,

$$P(\Delta a_N^{\text{meas}} \leq \Delta a_N^{\text{sim}} - \epsilon) = F_{\text{meas}}(\Delta a_N^{\text{sim}} - \epsilon)$$

Similarly, the first term on the right-hand side of Eq. (16) can be written as

$$P(d + \epsilon \geq 0) = \int_{\Delta a_N^{\text{sim}}} P(\Delta a_N^{\text{sim}} - \Delta a_N^{\text{meas}}$$

$$+ \epsilon \geq 0) f_{\text{sim}}(\Delta a_N^{\text{sim}}) \, d\Delta a_N^{\text{sim}}$$

$$= \int_{\Delta a_N^{\text{sim}}} F_{\text{meas}}(\Delta a_N^{\text{sim}} + \epsilon) f_{\text{sim}}(\Delta a_N^{\text{sim}}) \, d\Delta a_N^{\text{sim}} \quad (18)$$

Thus, by combining Eqs. (17) and (18), the likelihood can be written as

$$l(\Delta a | m) = \int_{\Delta a_N^{\text{sim}}} [F_{\text{meas}}(\Delta a_N^{\text{sim}} + \epsilon)$$

$$- F_{\text{meas}}(\Delta a_N^{\text{sim}} - \epsilon)] f_{\text{sim}}(\Delta a_N^{\text{sim}}) \, d\Delta a_N^{\text{sim}}$$

$$\approx 2\epsilon \int_{\Delta a_N^{\text{sim}}} f_{\text{meas}}(\Delta a_N^{\text{sim}}) f_{\text{sim}}(\Delta a_N^{\text{sim}}) \, d\Delta a_N^{\text{sim}} \quad (19)$$

where the central finite difference approximation is used in the second relation, which becomes exact when $\epsilon \to 0$. As explained before, since the posterior PDF will be normalized, the coefficient 2ϵ can be ignored. The above expression in particular is convenient for separable MCS, because the analytical expression of $f_{\text{meas}}(x)$ is known, and $f_{\text{sim}}(x)$ can be evaluated by propagating uncertainty through numerical simulation. Let M be the number of samples in MCS; the likelihood can then be calculated by

$$l(\Delta a | m) = \int_{\Delta a_N^{\text{sim}}} f_{\text{meas}}(\Delta a_N^{\text{sim}}) f_{\text{sim}}(\Delta a_N^{\text{sim}}) \, d\Delta a_N^{\text{sim}}$$

$$\approx \frac{1}{M} \sum_{i=1}^{M} f_{\text{meas}}(\Delta a_{N,i}^{\text{sim}}) \quad (20)$$

First, input random samples such as noise and pressure are generated according to their distribution types. These input random samples are propagated through the Paris model to produce samples of crack growth Δa_N^{sim}. Second, the values of PDF $f_{\text{meas}}(\Delta a_N^{\text{sim}})$ are evaluated for all samples, whose average is the likelihood. The numerical experiments showed that $M = 2000$ is enough to obtain a smooth distribution of the likelihood function. Note that likelihood calculation is computationally intensive, because Eq. (20) needs to be evaluated for every m in the range of Eq. (8). In addition, the Bayesian inference in Eq. (8) is repeated at every inspection cycle.

Once the posterior distribution of m is obtained from Bayesian inference, it can be used to estimate the RUL, which is the expected life from the current cycle to the failure. In this paper, the failure is defined as when the crack size reaches the critical crack size a_C in Eq. (6). From Eq. (5), the RUL can be estimated by

$$N_f = \frac{a_C^{1-\frac{m}{2}} - (a_N^{\text{sim}})^{1-\frac{m}{2}}}{C(1 - \frac{m}{2})(\sigma(\sqrt{\pi}))} \quad (21)$$

Note that the RUL, N_f, is also randomly distributed. Thus, it only makes sense to estimate the RUL as a distribution. The distributions of m and σ are given from Bayesian inference and Eq. (3), respectively. Although the true crack size, a_N^{true}, should be a deterministic value, it has to be estimated from the measured crack size, a_N^{meas}. Thus, it needs to be considered as a random variable. For the given noise and bias model, the true crack size can be estimated by

$$a_N^{\text{true}} \sim U(a_N^{\text{meas}} - b/2 - V/2; a_N^{\text{meas}} - b/2 + V/2) \quad (22)$$

The distribution of RUL is calculated at every inspection cycle using MCS with 50,000 samples. Since predicting RUL is an extrapolation process, the input uncertainties are amplified in
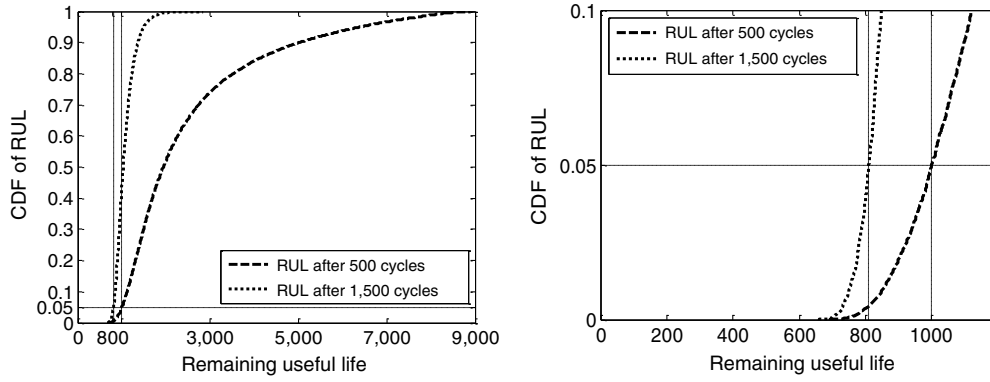
Fig. 2 Cumulative distribution function of RUL after updating the distribution of damage growth parameter m using Bayesian inference.

predicting uncertainty in RUL. To predict the RUL safely, we choose fifth percentile as a conservative estimate of RUL.

Figure 2 shows an example of predicted CDF of RUL of a panel under cyclic uniform stress with initial half-crack size of 10 mm after 500 and 1500 cycles. The total life of the structure is about 2500 cycles if mean values of all input parameters are used. It can be observed that the estimated mean values of RUL are about 2000 and 1000 after 500 and 1500 cycles, respectively. However, these mean values would provide about 50% chance of overpredicting the RUL for given uncertainties in input parameters and SHM measurements. To have a 95% conservative estimate, we choose the CDF value of 0.05, which corresponds to 1000 and 800 cycles, respectively, (two vertical lines in Fig. 2). At 500 cycles, the conservative RUL estimate has ratio of 0.5 (1000/2000) compared to the mean RUL, while at 1500 cycles the ratio becomes 0.8 (800/1000). This happens because the knowledge on damage growth parameter m is improved through Bayesian inference: i.e., the uncertainty in m is reduced.

IV. Numerical Application

In this paper, synthetic SHM measurements are used to demonstrate the process of Bayesian inference and predicting RUL. Depending on manufacturing and assembly processes, the actual damage growth parameters for individual aircraft can be different. For a specific panel, it is assumed that there exists a true value of deterministic damage growth parameters ($m_{\text{true}} = 3.8$ and $C_{\text{true}} = 1.5 \times 10^{-10}$). In the following numerical simulation, the true damage will grow according to the true values of damage growth parameters. On the other hand, the measured damage size will have bias and noise from measurements. To simplify the presentation, the distributions of m and C are considered separately, which means that when one variable is uncertain, the other one is assumed to be known with its true value.

Table 1 Geometry, loading, and damage growth parameters of 7075-T651 aluminum alloy

Property	Distribution type
Radius of fuselage r, m	Deterministic 3.25
Thickness of panel t, m	Deterministic 0.00248
Pressure differential Δp, MPa	Lognormal (0.06,0.003)[a]
Fracture toughness K_{IC}, MPa$\sqrt{\text{meter}}$	Deterministic 30
Critical half-crack size, a_C, m	0.0463
True damage growth parameter m_{true}	3.8
True damage growth parameter C_{true}	1.5E − 10
Initial distribution of m	Uniform (3.3, 4.3)[b]
Initial distribution of $\log(C)$	Uniform (log(5E − 11), log(5E − 10))
Noise v, mm	Uniform (−V, +V), V = 1.0, or 3.0
Bias b, mm	Deterministic, −2.0, 0.0, or 2.0

[a]Lognormal (mean, standard deviation), modeled as constant in simulations.
[b]Uniform (lower bound, upper bound).

Typical material properties for 7075-T651 aluminum alloy are presented in Table 1. The applied fuselage pressure differential is 0.06 MPa [26], and the stress is given by Eq. (3). Paris model parameters m and C are obtained using a crack growth rate plot [27]. Note that due to scatter of the crack growth rate, the exponent m and $\log(C)$ are assumed to be uniformly distributed between the lower and upper bounds.

From the preliminary damage growth analysis, it was found that the distribution of pressure p has negligible effect on damage growth, because the effect of randomness is averaged out. Thus, in the following analysis, the applied pressure is assumed to be deterministic, 0.06 MPa, which is the mean of the distribution obtained from Niu [26].

In general, the minimum size of detectable damage using SHM is much larger than that of the manual inspection. Although different SHM techniques may have different minimum detectable size, we chose an initial half-crack size of $a_0 = 10$ mm, which is large enough to be detected by most ultrasonic diagnostic methods in SHM. In addition, this size of damage will provide significant crack growth data between two consecutive inspections.

In the following sections, two cases are considered. The first is updating parameter m, and the second is updating parameter C. First, one set of measured crack sizes is generated at every SHM measurement interval ΔN by adding noise and bias to the true crack sizes that are calculated from the Paris model [see Eqs. (5) and (9)]. Then at every measurement interval, Bayesian inference is used to update the PDF of m. Once the PDF of m is available, Eq. (21) is used to estimate the distribution of RUL of which its fifth percentile is used as a conservative estimate of RUL. Since synthetic data are used by adding random noise, the result may vary with different sets of samples. Thus, the above process is repeated with 100 sets of measurements and the mean $\pm$ 1 standard deviation intervals are plotted. Figure 3 shows a flowchart of calculating likelihood function using Monte Carlo simulation.

Input data: $a_{N-2\Delta N}^{meas}$, Δa_N^{meas}

Discretize $\boldsymbol{m} = [m_1, m_2, \cdots, m_n]$

Loop for every m_i:

Generate M samples of $\left(a_{N-2\Delta N}^{sim}\right)_j = a_{N-2\Delta N}^{meas} + v_j$ with $v_j \sim U(-V, V)$

Simulated crack sizes: $\left(a_{N-\Delta N}^{sim}\right)_j = \left[\Delta N C \left(1 - \frac{m_i}{2}\right)\left(\sigma\sqrt{\pi}\right)^{m_i} + \left(a_{N-2\Delta N}^{sim}\right)_j^{1-\frac{m_i}{2}}\right]^{\frac{2}{2-m_i}}$

Simulated crack sizes: $\left(a_N^{sim}\right)_j = \left[2\Delta N C \left(1 - \frac{m_i}{2}\right)\left(\sigma\sqrt{\pi}\right)^{m_i} + \left(a_{N-2\Delta N}^{sim}\right)_j^{1-\frac{m_i}{2}}\right]^{\frac{2}{2-m_i}}$

Simulated crack growth: $\left(\Delta a_N^{sim}\right)_j = \left(a_N^{sim}\right)_j - \left(a_{N-\Delta N}^{sim}\right)_j$

Likelihood: $l(\Delta a | m_i) = \frac{1}{M}\sum_{j=1}^{M} f_{meas}\left(\Delta a_N^{sim}\right)_j$

End loop

Fig. 3 Flowchart of calculating likelihood function using Monte Carlo Simulation.
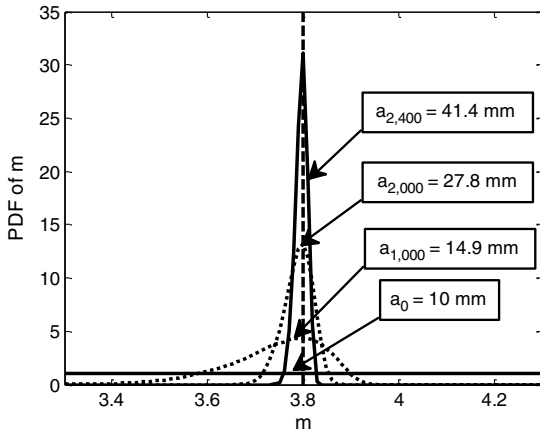
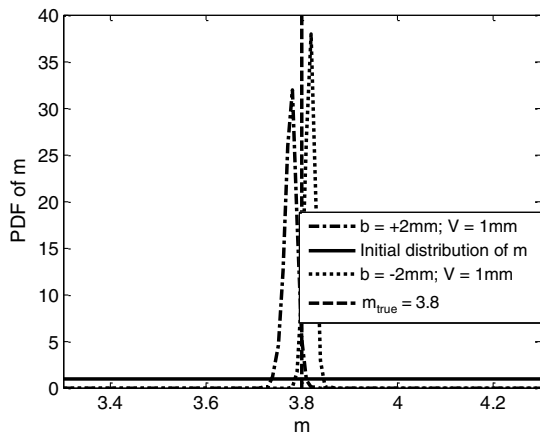Fig. 4   Updated probability density functions of *m*.
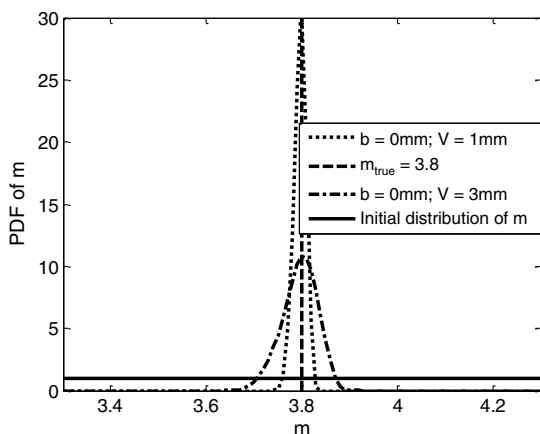

Fig. 5   Effect of bias on updated PDF of *m*.

Fig. 6   Effect of noise on the updated PDF of *m*.

V.   Updating Damage Growth Parameter *m*

In this section, it will be shown that the distribution of the damage growth parameters for a fuselage panel is narrowed using SHM measurement data and Bayesian inference. It is assumed that initially the panel has a 20 mm through-the-thickness crack that is monitored by SHM equipment. Although some SHM methods can detect small cracks, 20 mm is chosen because it is a reasonable size that can be detectable using most SHM equipments in the field. The true crack grows according to damage growth parameters m_{true} and C_{true} in Table 1.

It is assumed that SHM measurements are performed at every 100 cycles (i.e., $\Delta N = 100$). Since the crack grows slowly and the noise and bias of measurements are, in general, large, overly frequent measurements may not provide significant information about the crack growth. The synthetic measured crack size data are generated by adding random noise and deterministic bias to the true crack size data. In the following Bayesian inference, only the measured crack size data are used.

As an example, the parameter *m* will be updated, while the true value C_{true} of the parameter *C* is assumed to be known. Starting from the initial uniform distribution, the PDF of *m* is progressively updated using Bayesian inference with measured damage sizes. The noise in crack detection is assumed to be uniform $(-1, +1 \text{ mm})$ and the bias is assumed to be zero. SHM measurements are conducted until the crack reaches its half critical size a_C, defined in Eq. (6) with a value of about 42.7 mm. Figure 4 plots the updated PDFs of *m* at every 1000 cycles. It is clear that as the crack grows, the PDF of *m* becomes narrower and it converges to the true value of $m_{\text{true}} = 3.8$. It is noted that the convergence becomes faster as the crack size increases, because the crack growth is faster for a larger crack.

Figure 5 shows the effect of bias on the final updated PDF of *m*. The noise in crack detection is assumed to be uniform $(-1, +1)$ and two different biases are used: $b = -2$ and 2 mm. It is clear that bias shifts the maximum likelihood point (the peak of PDF) from that of the true value; the negative bias overestimates the PDF of *m*, while the positive bias underestimates it. Even if bias cause a shift in the distribution, its effect is insignificant in estimating RUL. Bayesian inference over/underestimate the distribution so that the predicted damage size is close to the measured one. In other words, Bayesian inference tried to compensate the model error by shifting the distribution.

Figure 6 shows the effect of noise on the PDF of *m* when $b = 0$ mm. It is obvious that noise has an effect on the standard deviation but does not shift the distribution as the bias does. The smaller the noise, the narrower the final PDF of *m*.

Table 2 shows statistical characteristics, such as the maximum likelihood, mean and standard deviation of PDF of *m*, corresponding to Figs. 5 and 6. It can be observed that the mean and maximum likelihood values are minimally affected by the bias and noise. However, the standard deviation increases with a large noise. As expected, a positive bias (true crack size is smaller than the measured one) leads to an underestimation of *m*.

Once the PDF of *m* is obtained, it can be used to predict the RUL of the monitored panel. Since the PDF is updated at every SHM measurement, the predicted RUL will vary at every measurement interval ΔN. In predicting RUL, 50,000 samples of *m*, a_N^{true}, and σ are generated, and Eq. (21) is used to calculate samples of N_f. To have a safe prediction of RUL, the fifth percentile of N_f samples is used as a conservative estimate of RUL. Since we used synthetic data by adding random noise, the result may vary with different sets of data.

Table 2   Statistical characteristics of final PDF of with different combinations of bias/noise

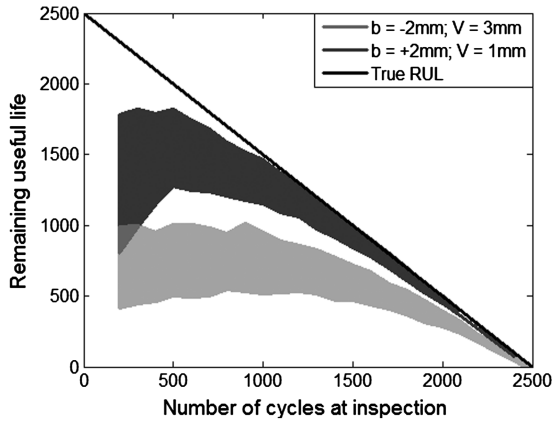| Bias, noise, mm	Effect of noise		Effect of bias	
	$b = 0, V = 1$	$b = 0, V = 3$	$b = -2, V = 1$	$b = +2, V = 1$
Max. likelihood	3.80	3.80	3.82	3.78
Mean	3.80	3.80	3.82	3.78
Standard deviation	0.01	0.04	0.01	0.01

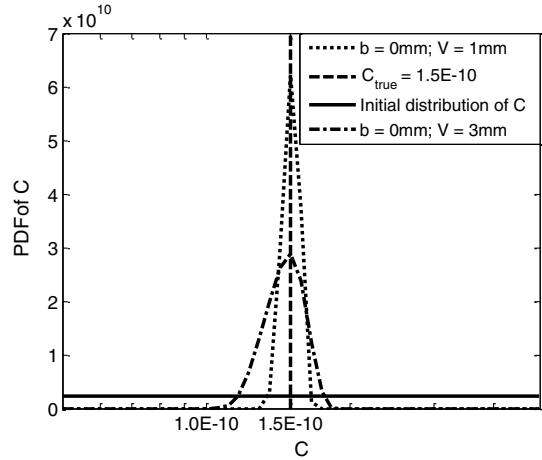**Fig. 7 One-sigma intervals of 95% conservative RUL compared to the true RUL.**

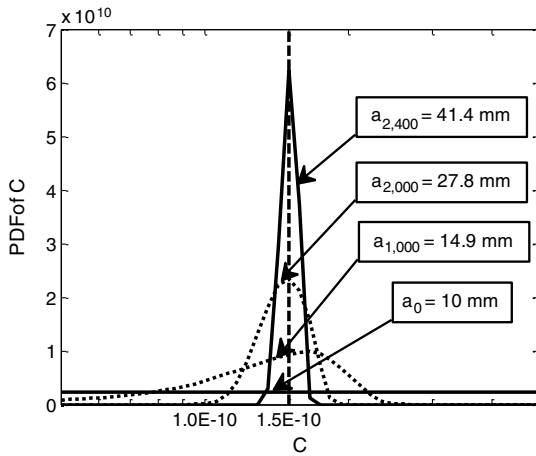**Fig. 10 Effect of noise on final PDF of m.**

Fig. 8 Updated probability density functions of $\log(C)$.
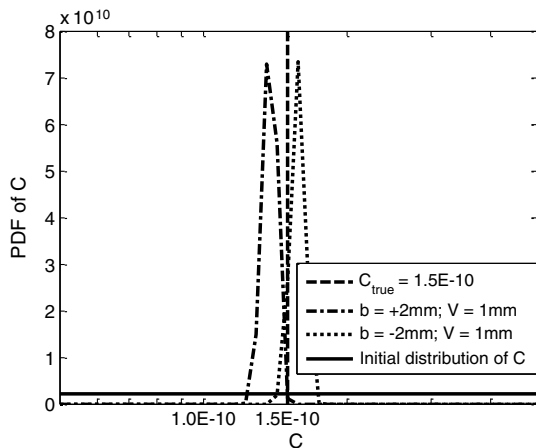

Fig. 9 Effect of bias on the updated PDF of $\log(C)$.

Thus, the above process is repeated with 100 sets of measurement data, and mean ± 1 standard deviation intervals are plotted. Figure 7 shows these conservative intervals of RUL with two different combinations of noise and bias. These combinations correspond to extreme cases; the most and least conservative estimates of RUL. To compare the predicted RUL with true one, the true RUL is also plotted in the figure. Note that initially the difference between the true and predicted RULs is significant, because uncertainty is large at an early stage. However, the predicted RUL converges to the true one from the safe side as more numbers of updates are performed. In addition, the variability of estimated RUL is also gradually reduced. Thus, it can be concluded that the proposed Bayesian inference can estimate panel-specific damage growth parameters as well as the RUL while maintaining conservative.

VI. Updating Damage Growth Parameter C

In this section, as a second example, the damage growth parameter C is updated, while $m = m_{\text{true}}$ is used, starting from the initial distribution given in Table 1. Since the Paris model is linear in a log–log scale and since C is the y intercept at $\Delta K = 1$, $\log(C)$ is updated instead of C. The updating process is the same as updating the distribution of m described in Sec. V with the same type of likelihood function and the same noise and bias. Starting from the initial uniform distribution, the PDF of $\log(C)$ is progressively updated using Bayesian inference with measured damage sizes. The noise in crack detection is assumed to be uniform $(-1, +1)$ and the bias to be zero. SHM measurements are conducted until the crack reaches its half critical size, a_C. Figure 8 plots the updated PDFs of $\log(C)$ at every 1000 cycles. It is clear that as the crack grows, the PDF of $\log(C)$ becomes narrower and it converges to the true value of $C_{\text{true}} = 1.5 \times 10^{-10}$. It is noted that the convergence becomes faster as the crack size increases, because the crack growth is faster for a larger crack.

The effects of noise and bias turn out to be similar to the case of updating m. Figure 9 shows the effect of bias on the final updated PDF of $\log(C)$. The noise in crack detection is assumed to be uniform $(-1, +1)$ and two different biases are used: $b = -2$ and 2 mm. As for m, bias appears to shift the maximum likelihood point from that of the true value; the negative bias overestimates the PDF of $\log(C)$, while the positive bias underestimates it.

Figure 10 shows the effect of noise on the PDF of $\log(C)$ when $b = 0$ mm. It is obvious that noise increases the standard deviation

Table 3 Statistical characteristics of updated PDF of $\log(C)$ with different combinations of bias/noise

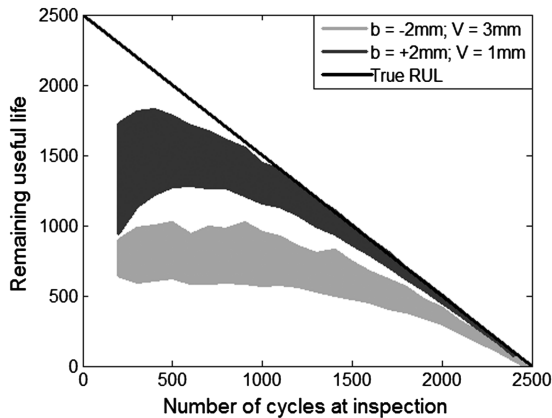| Bias, noise, mm	Effect of noise		Effect of bias	
	$b = 0, V = 1$	$b = 0, V = 3$	$b = -2, V = 1$	$b = +2, V = 1$
Max. likelihood	$1.5E - 10$	$1.5E - 10$	$1.6E - 10$	$1.4E - 10$
Mean	$1.5E - 10$	$1.5E - 10$	$1.6E - 10$	$1.4E - 10$
Standard deviation	$5.9E - 12$	$1.3E - 11$	$5.3E - 12$	$6.0E - 12$

Fig. 11   One-sigma intervals of 95% conservative RUL compared to the true RUL.

but it does not shift the distribution as the bias does. The smaller the noise, the narrower the final PDF of $\log(C)$.

Table 3 shows statistical characteristics, such as the maximum likelihood, mean and standard deviation of PDF of C, corresponding to Figs. 9 and 10. It can be observed that the mean is only minimally affected by the bias and noise in the data. However, the standard deviation is large with large noise. As expected, positive bias (true crack size is smaller than measured) leads to an underestimation of C. From Figs. 9 and 10, it can be concluded that the effects of noise and bias are similar to updating both m and C.

Similar to the case of updating m, the predicted RULs from the updated $\log(C)$ at every measurement interval are plotted in Fig. 11. Again, it is clear that the conservative estimate of RUL approaches the true RUL from the safe side. In addition, the variability of estimated RUL is also gradually reduced. Thus, it can be concluded that the proposed Bayesian inference can estimate panel-specific damage growth parameters as well as predict the RUL while maintaining conservative.

VII.   Conclusions

In this paper, a Bayesian inference method is employed to identify panel-specific damage growth parameters using damage sizes measured from SHM sensors. The actual measurement environment is modeled by introducing deterministic bias and random noise. The likelihood function is calculated by comparing measured crack growth with simulated crack growth, which requires uncertainty propagation though the physics model that governs the crack growth. Because of many uncertainties involved, the RUL is predicted statistically and uses 95% conservative estimation.

Through numerical examples, it is shown that the probability distributions of the two damage growth parameters m and C are effectively narrowed and converged to the true values. The large number of SHM data compensates for the effect of noise, and thus the identified damage growth parameters are relatively insensitive to it. However, the effect of bias remains, and it affects the identification of true damage growth parameters. It is shown that convergence is slow when the bias is negative and noise is large, while it is fast when the bias is positive and the noise is small. However, the latter yields an underestimation of the true parameters.

The identified distributions of parameters are used to estimate the RUL with 95% confidence. In all combined cases with noise and bias, the proposed method converges to the true RUL from the conservative side.

In the more general approach, it is possible to update both m and C using their joint PDF. In addition, the unknown bias can also be considered as an uncertain variable and can be updated together. However, as the number of variables increases, the computational cost increases significantly, because the proposed method is based on MCS for uncertainty propagation. In the future, the possibility of reducing computational cost by using surrogate modeling techniques will be investigated.

References

[1]   Wang, L., and Yuan, F. G., "Damage Identification in a Composite Plate Using Prestack Reverse-Time Migration Technique," *Structural Health Monitoring*, Vol. 4, No. 3, 2005, pp. 195–211.
      doi:10.1177/1475921705055233

[2]   Luo, J., Namburu, M., Pattipati, K., Qiao, L., Kawamoto, M., and Chigusa, S., "Model-Based Prognostic Techniques [Maintenance Applications]," *IEEE Systems Readiness Technology Conference*, Inst. of Electrical and Electronics Engineers, Piscataway, NJ, 2003, pp. 330–340.

[3]   Li, C. J., and Lee, H., "Gear Fatigue Crack Prognosis Using Embedded Model, Gear Dynamic Model and Fracture Mechanics," *Mechanical Systems and Signal Processing*, Vol. 19, 2005, pp. 836–846.
      doi:10.1016/j.ymssp.2004.06.007

[4]   Berruet, P., Toguyeni, A., K. A., and Craye, E., "Structural and Functional Approach for Dependability in FMS," *IEEE International Conference on Systems, Man, and Cybernetics*, Vol. 4, Inst. of Electrical and Electronics Engineers, Piscataway, NJ, 1999, pp. 481-485.
      doi:10.1109/ICSMC.1999.812452

[5]   Ray, A., and Patankar, R., "A Stochastic Model of Fatigue Crack Propagation Under Variable-Amplitude Loading," *Engineering Fracture Mechanics*, Vol. 62, 1999, pp. 477–493.
      doi:10.1016/S0013-7944(98)00103-9

[6]   Ray, A., and Tangirala, S., "Stochastic Modeling of Fatigue Crack Dynamics for Online Failure Prognostics," *IEEE Transactions on Control Systems Technology*, Vol. 4, 1996, pp. 443–451.
      doi:10.1109/87.508893

[7]   Law, L. C., "Neural Networks for Model-Based Prognostics," *IEEE Aerospace Conference*, Vol. 3, Inst. of Electrical and Electronics Engineers, Piscataway, NJ, 1999.
      doi:10.1109/AERO.1999.789761

[8]   Schwabacher, M. A., "A Survey of Data-Driven Prognostics," AIAA Infotech@Aerospace Conference, AIAA Paper 2005-7002, 2005.

[9]   Montanari, G. C., "Aging and Life Models for Insulation Systems Based on PD Detection," *IEEE Transactions on Dielectrics and Electrical Insulation*, Vol. 2, 1995, pp. 667–675.
      doi:10.1109/94.407031

[10] Xue, Y., McDowell, D. L., Horstemeyer, M. F., Dale, M. H., and Jordon, J. B., "Microstructure-Based Multistage Fatigue Modeling of Aluminum Alloy 7075-T651," *Engineering Fracture Mechanics*, Vol. 74, 2007, pp. 2810–2823.
      doi:10.1016/j.engfracmech.2006.12.031

[11] Goebel, K., Saha, B., and Saxena, A., "A Comparison of Three Data-Driven Techniques for Prognostics," *62nd Meeting of the Society for Machinery Failure Prevention Technology (MFPT)*, 2008, pp. 119–131.

[12] Srivastava, A. N., and Das, S., "Detection and Prognostics on Low Dimensional Systems," *IEEE Transactions on Systems, Man, and Cybernetics*, Pt. C, Vol. 39, 2009, pp. 44–54.
      doi:10.1109/TSMCC.2008.2006988

[13] Tipping, M., "The Relevance Vector Machine. in Advances in Neural Information Processing Systems," MIT Press, Cambridge, MA, 2000.

[14] Yan, J., and Lee, J., "A Hybrid Method for On-line Performance Assessment and Life Prediction in Drilling Operations," *IEEE International Conference on Automation and Logistics*, Inst. of Electrical and Electronics Engineers, Piscataway, NJ, 2007, pp. 2500-2505.

[15] Orchard, M., Kacprzynski, G., Goebel, K., Saha, B., and Vachtsevanos, G., "Advances in Uncertainty Representation and Management for Particle Filtering Applied to Prognostics," *International Conference on Prognostics and Health Management*, Prognosis and Health Management Society, 2008, pp. 1–6.

[16] Sheppard, J. W., Kaufman, M. A., Inc, A., and Annapolis, M. D., "Bayesian Diagnosis and Prognosis Using Instrument Uncertainty," *IEEE Autotestcon*, Inst. of Electrical and Electronics Engineers, Piscataway, NJ, 2005, pp. 417–423.

[17] Saha, B., and Goebel, K., "Uncertainty Management for Diagnostics and Prognostics of Batteries Using Bayesian Techniques," *IEEE Aerospace Conference*, Inst. of Electrical and Electronics Engineers, Piscataway, NJ, 2008, pp. 1–8.
      doi:10.1109/AERO.2008.4526631

[18] Engel, S. J., Gilmartin, B. J., Bongort, K., and Hess, A., "Prognostics: The Real Issues Involved with Predicting Life Remaining," *IEEE Aerospace Conference*, Vol. 6, Inst. of Electrical and Electronics Engineers, Piscataway, NJ, March 2000, pp. 456–467.
doi:10.1109/AERO.2000.877920

[19] Gu, J., Barker, D., and Pecht, M., "Uncertainty Assessment of Prognostics of Electronics Subject to Random Vibration," *AAAI Fall Symposium on Artificial Intelligence for Prognostics*, AIAA, Reston, VA, 2007, pp. 50–57.

[20] Orchard, M., Wu, B., and Vachtsevanos, G., "A Particle Filter Framework for Failure Prognosis," World Tribology Congress III, Washington, D.C., Paper WTC2005-64005, Sept. 2005.

[21] Paris, P. C., Tada, H., and Donald, J. K., "Service Load Fatigue Damage—A Historical Perspective," *International Journal of Fatigue*, Vol. 21, 1999, pp. 35–46.
doi:10.1016/S0142-1123(99)00054-7

[22] Harkness, H. H., "Computational Methods for Fracture Mechanics and Probabilistic Fatigue," Ph.D. Thesis, Northwestern Univ., Evanston, IL, 1994.

[23] Lin, K. Y., Rusk, D. T., and Du, J. J., "Equivalent Level of Safety Approach to Damage-Tolerant Aircraft Structural Design," *Journal of Aircraft*, Vol. 39, 2002, pp. 167–174.
doi:10.2514/2.2911

[24] An, J., Acar, E., Haftka, R. T., Kim, N. H., Ifju, P. G., and Johnson, T. F., "Being Conservative with a Limited Number of Test Results," *Journal of Aircraft*, Vol. 45, 2008, pp. 1969–1975.
doi:10.2514/1.35551

[25] Smarslok, B. P., Alexander, D., Haftka, R. T., Carraro, L., and Ginsbourger, D., "Separable Monte Carlo Applied to Laminated Composite Plates Reliability," 49th AIAA/ASME/ASCE/AHS/ASC Structures, Structural Dynamics, and Materials Conference, Schaumburg, IL, AIAA Paper 2008-17512008.

[26] Niu, M., "Airframe Structural Design," *Fatigue, Damage Tolerance and Fail-Safe Design*, Conmilit, Hong Kong, 1990, pp. 538–570.

[27] Newman, J. C., Phillips, E. P., and Swain, M. H., "Fatigue-Life Prediction Methodology Using Small-Crack Theory," *International Journal of Fatigue*, Vol. 21, 1999, pp. 109–119.
doi:10.1016/S0142-1123(98)00058-9